Evaluation of Transmission Line Fault Location Feasibility By Using M-Class PMUs: Real-World Case Studies in the Brazilian Power Network

Felipe V. Lopes, Arthur Mouco, Rafael O. Fernandes, and Felipe C. Neto

***Abstract*—Transmission line fault location is of paramount importance to speed up the power system restoration after outages. Among the existing fault location methods, the most widespread are those based on fundamental phasors, whose estimations must converge to the fault steady-state regime before the line circuit breakers open. Thereby, traditional fault locators usually consider phasor estimations obtained from protective relays or P-class Phasor Measurement Units, which present filtering latency times shorter than those of M-class Phasor Measurement Units. However, although it is commonly assumed that M-class phasor samples are not suitable for fault location applications due to their intrinsic filtering delay, studies on the feasibility of M-class data-based fault location applications are not yet available in the literature. Therefore, this work aims to investigate if M-class Phasor Measurement Units could be used in real fault location schemes, taking advantage of already deployed measurement systems. To do so, actual fault events occurred on the Brazilian power grid are analyzed, and the performance of four different phasor-based fault location algorithms are evaluated when phasor samples obtained from a traditional protective relay algorithm and from M-class Phasor Measurement Units are used as inputs. Unlike the preliminary expectations, the obtained results highlight evidences that M-class phasor measurements can be used in fault location applications, since they resulted in errors within the expected levels for phasor-based fault location methods.**

***Keywords*—Fault location, Phasor Measurement Units, power systems, real-world records, transmission lines.**

I. Introduction

CALCULATING the fault location (FL) on power networks have been a task of great importance for utilities to speed up line restoration procedures after faults [1]. Various FL schemes have been applied in real systems, among which the phasor-based fault location (PHFL) techniques are still the most widespread [2]. These solutions require voltage and current fundamental phasors to be estimated, whose values are then used as inputs of FL estimation formulas.

Felipe V. Lopes is with the Department of Electrical Engineering at Federal University of Paraíba (UFPB), 58051-900, Campus I, João Pessoa-PB, Brazil. (e-mail: felipelopes@cear.ufpb.br).

Arthur Mouco is with the Brazilian Independent System Operator (ONS), 251 Júlio do Carmo St., Cidade Nova, Rio de Janeiro, Brazil, 20211-160 (e-mail: arthurdcm@hotmail.com).

Rafael O. Fernandes is with Unicamp, Av. Doutor Gastão Vidigal, 1132, Apto 206B, Vila Leopoldina, São Paulo, 05314-001 (e-mail: r096443@dac.unicamp.br).

Felipe C. Neto is with Furnas Centrais Elétricas, Av. Graça Aranha, 26, Centro, Rio de Janeiro, Brazil, 20030-000 (e-mail: fcamara@furnas.com.br).

Paper submitted to the International Conference on Power Systems Transients (IPST2021) in Belo Horizonte, Brazil June 06-10, 2021.

In today's technology, micro-processed line monitoring devices usually compute phasors by means of Discrete Fourier Transform (DFT) inspired solutions, which analyze signal samples stored in data windows [3]. Thus, when a power system passes from its normal operation to a fault condition, i.e., as soon as the fault takes place, the data window starts to store pre-fault and fault period samples. It yields erroneous phasor estimations until the transition period is over, i.e., until the window is completely fulfilled by fault period samples, so that the time required by phasors to converge to the fault steady-state regime depends on the data window length [3].

Short data windows result in a quick phasor convergence, but they present a relatively poor filter frequency response. On the other hand, long data windows guarantee more accurate phasor estimations, but slower response times are observed [4]. Since protective relays must operate in real-time detecting faults as soon as possible, protection functions typically apply one-cycle window-based phasor estimations algorithms [3]. Hence, in PHFL methods, FL must be computed within a valid calculation period that begins after the data window transition time (≈ 1 cycle after the fault inception), and ends when the line circuit breakers (CBs) open [5]. Thus, PHFL devices must be fast enough to converge to the fault steady-state FL values before the CBs isolate the faulted section, otherwise, locating the fault may not be possible. Even though, it should be known that speeding up the phasor estimation process can decrease the accuracy of calculated fundamental components [3], which can affect the PHFL performance as well.

Still considering the above-mentioned context, it is worthy to mention that Phasor Measurement Units (PMUs) have gained importance over the years, being increasingly used in power networks to improve their observability and controllability. PMUs operate following the IEEE C37.118.1 standard requirements [6], resulting in more accurate phasor estimations than those obtained from traditional relays. This feature has motivated several PMU-based applications [7], among which PHFL functions stand out [8]–[11].

To improve the phasor estimation accuracy, PMUs apply additional filtering steps [12], which increase the phasor measurement response time in relation to those verified in protective relays [13]. M-class PMUs apply more filtering than P-class units, because they are intended for applications that require higher rejection to off-nominal frequency signals [14]. Thus, they present slower convergence [15], leading them to be usually disregarded in applications supposed to require short step response times [16], such as PHFL approaches.

Although several works report PMU-based PHFL solutions [8]–[11], recommendations regarding the use of P or M-class data are not explicitly reported in most literature references. As an exception, in [8], it is stated that "P-class data makes accurate fault location possible", but from the authors' best knowledge, detailed investigations about the feasibility of PHFL procedures based on M-class measurements had never been reported in the open literature. Indeed, since there is a preliminary expectation that M-class phasors may not converge to the fault steady-state values before the faulted line CBs open, the concept that M-class data should be avoided in PHFL applications have been accepted. Thereby, M-class PMUs are often disregarded in PHFL schemes, even in power systems in which M-class PMUs are widely available.

Aiming to improve line monitoring applications, several utilities worldwide have demonstrated great interest in expanding applications based on data taken from existing measurement networks. Thus, in this paper, an innovative study is presented with the objective to verify whether PHFL methods can provide reliable fault distance estimations while using M-class PMU data. For this study, real fault measurements taken from the Brazilian power grid are analyzed. FL is calculated via four different PHFL methods, whose results are evaluated and compared when two types of phasor measurements are considered as inputs: 1) M-class PMU phasors; and 2) protective relay phasors. The results demonstrate that reliable PHFL estimations can be obtained by using M-class PMU data, despite the larger measurement response time they have in relation to P-class PMUs and traditional protective relays.

II. PMUs Fundamentals

A. *PMU Phasor-Estimation Process*

The PMU was invented in mid-1980s [7], and it brings advantages over traditional phasor measurement systems. As reported in [6], PMUs measure three-phase voltages and currents in complex polar form, using typical measurement rates that range from 10 to 60 phasor samples/second (although new technologies can reach up to 240 samples/second). Also, it takes advantage of a satellite-based radio-navigation system (e.g. GPS, GLONASS, Galileo, etc.), so that PMU measurements are tagged with an universal time-stamp. As a result, estimated phasors are time synchronized wherever the PMUs are placed [7], which facilitates multi-terminal applications in which an unique time reference is required.

Although the features of PMUs from different vendors can present slight variations, the overall phasor estimation process usually follows the same steps. To explain the main PMU characteristics, the generic architecture reported in [12] is considered, which is shown in Fig. 1. For the sake of objectivity, only the steps associated to the phasor estimation process are described next:

- **Step 1) Anti-Aliasing Filter:** It avoids the aliasing effect during the input signals sampling. It consists in an analog low-pass Butterworth filter, usually of 2nd or 3rd order [3], with cutoff frequency that depends on the sampling rate used, complying the Nyquist criterion.
- **Step 2) A/D Converter:** It is responsible to digitize the analyzed analog signals into discrete waveform samples separated in time by a given sampling period. Sampling rates from 16 to 64 samples per cycle (fixed at the power system nominal frequency) are commonly used [3].
- **Step 3) Phasor Estimation:** It is usually carried out using solutions inspired in the recursive DFT algorithm, through which phasors are computed from signal samples stored typically in an one-cycle time sliding data window. Since the windowing process is an issue from the point of view of spectral estimation, in some PMUs, other window types than the traditional rectangular one can be used [3].
- **Step 4) Digital Filtering:** System frequency variations can lead data windows (employed in the Step 3) to encompass a number of samples that does not match exactly a power cycle, even if frequency estimators are applied. As a result, a slope in the estimated phase angle may show up, and a (quasi) double-frequency component can take place in both estimated phasor angle and magnitude. Thereby, PMUs typically remove these errors by using additional digital filters, which can be implemented considering various schemes, among which the three-point averaging filter is often used [12].
- **Step 5) Post Processing:** In this step, the estimated quantities are compensated to correct attenuations introduced by the applied filtering procedures. Moreover, once all phasors have been calculated, they are decimated in accordance to the standard reporting rates [12], being then made available for control centers applications.

B. *PMU Classes and Time Response Issues*

As reported in [16], PMUs are typically divided into two classes of performance: P-class and M-class. P-class PMUs have shorter phasor estimation latency times, but they have lower harmonic component rejection requirements in comparison to the M-class PMUs. On the other hand, M-class devices apply more filtering to increase the phasor estimation quality, but with the drawback of having larger measurement convergence times during abruptly changes in monitored signals [15].

The above-mentioned considerations explain the reason that have led M-class PMUs to be usually disregarded in PHFL applications. Indeed, the PHFL algorithms require the evaluation of phasor samples within the fault steady-state period. Thus, FL estimations must be computed using samples

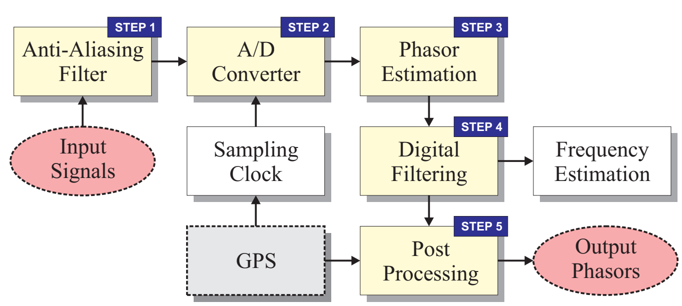

Fig. 1. PMU model structure.

taken from a valid calculation window, which starts after the phasor stabilization time and ends at the CBs opening instant [5]. Thereby, if the phasor estimation response time increases, but the CB opening time is not proportionally moved ahead on time, the FL computation window is narrowed, in such a way that phasor samples can never reach the required fault steady-state condition.

If phasors do not converge to the fault steady-state, the performance of PHFL methods can be jeopardized. Hence, PHFL methods traditionally use phasor samples taken from either protective relays or P-class PMUs, whose response times are usually short enough to assure the convergence of estimated phasors to the fault steady-state regime [5] (assuming that traditional one-cycle phasor-based relays and typical CBs are used).

To exemplify the above-mentioned issue, Fig. 2 compares the phasor magnitude obtained by means of a real M-class PMU and from a protective one-cycle data-based relay phasor estimation algorithm [17]. It is noticed that the PMU outputs are indeed more stable during the normal system operation, but a delayed convergence to the fault condition is observed in comparison to the relay response. As a consequence, as mentioned earlier, although M-class PMUs are widely available in several power systems, from the authors' best knowledge, neither they have been used for PHFL purposes nor studies on the effects of such delayed response on PHFL applications have been conducted. For example, M-class PMUs have been massively introduced throughout the Brazilian Interconnected Power System (BIPS) over the last years. Nevertheless, although the Brazilian PMU network is composed by 156 measurement M-class units up to date, as illustrated in Fig. 3, these devices have not been applied in PHFL schemes.

III. Case Studies

A. Evaluation Methodology

To evaluate the performance of PHFL when using PMU data, three real fault scenarios are studied. Only real records are considered in order to allow conclusions free of simulation modeling and simplifications issues, which could be questionable if simulated data were considered. The analyzed PMUs are M-class real devices, whose vendors are omitted for the sake of confidentiality. In order to compare the FL results obtained when traditional relay measurements are taken into account, data from real Digital Fault Recorders (DFRs) are also processed, emulating a relay phasor estimation process, which is implemented in this paper as reported in [17]. Hence, by having the control of this algorithm, a greater diversity of PHFL methods (including some which are not promptly available in real devices) could be tested, improving the comprehensiveness and clarity of the presented studies.

Fig. 4 depicts the applied evaluation methodology. Basically, $\widehat{V}_{PMU,abc}$ and $\widehat{I}_{PMU,abc}$ are obtained from real M-class PMUs installed in the analyzed systems, whereas the time-domain signals $v_{DFR,abc}$ and $i_{DFR,abc}$ are captured from real DFRs, also installed in the evaluated lines. Such DFR waveform

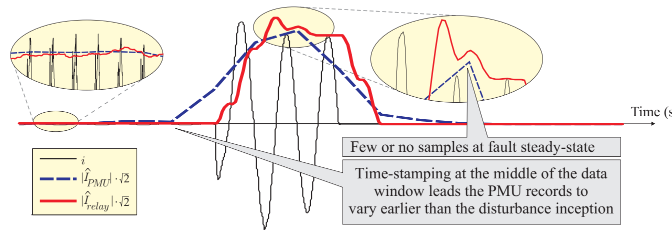

Fig. 2. M-class PMU and relay estimated phasor magnitude.

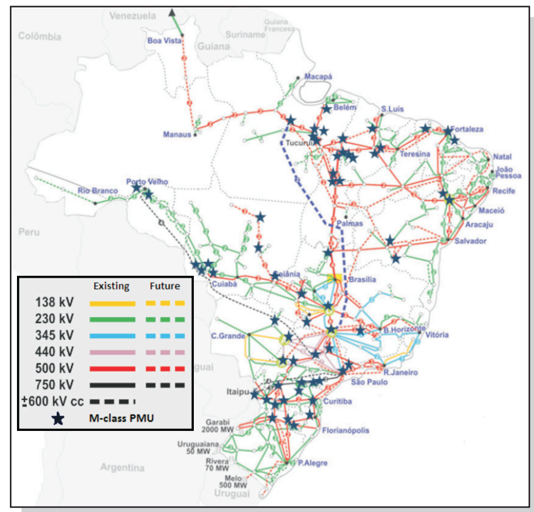

Fig. 3. PMU Deployment in the BIPS.

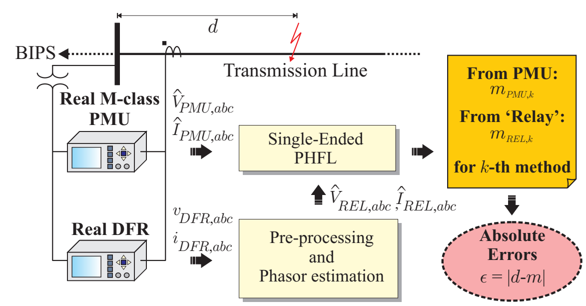

Fig. 4. Evaluation methodology.

samples are then pre-processed[1] and used as inputs in the relay phasor estimation algorithm, yielding $\widehat{V}_{REL,abc}$ and $\widehat{I}_{REL,abc}$. In a second step, the fault type estimated by the DFR is considered to select the correct fault loop to be analyzed by the evaluated PHFL methods, which are based on one terminal data. Also, the disturbance inception instant is detected, being the cycle-by-cycle method used to analyze PMUs magnitude samples [1], and the Park's transformation-based fault detection method reported in [18] applied to evaluate DFR signals. Regarding the latter method, it is worthy to mention that it was chosen because it is adaptive, so that threshold settings are not required, which allows a robust and accurate fault beginning identification.

[1] Since already discretized signals are taken into account, the pre-processing consists in a digital anti-aliasing filter with posterior downsampling to 16 samples/cycle, as adopted by several protective devices.

As a consecutive step, the fault distance d is estimated by means of four different single-ended PHFL methods, namely: Reactance method (REM) [2], Classical Takagi method (TKC) [19], Eriksson method (ERI) [20], and Wiszniewski method (WIS) [21]. Each technique is applied considering fundamental phasor samples obtained from the analyzed real M-class PMUs, resulting in $m_{PMU,k}$ fault distance estimations, and also considering measurements obtained from the relay phasor estimation algorithm, yielding the $m_{REL,k}$ FL estimations, being k=REM, TKC, ERI or WIS, depending on the used PHFL method. Hence, since all analyzed PHFL techniques are applied to both sources of phasor measurements (M-class PMU and relay algorithm), besides the evaluation of FL errors, the comparison between the PHFL results when M-class PMU and relay data are taken into account could be carried out as well, allowing the investigation of evidences on the M-class PMU-based FL feasibility, which consists in the main goal of this paper.

Since the real fault positions d reported by line maintenance crews are available for all cases, the obtained m estimations are compared to d. The absolute FL error ϵ is calculated for each case, for each line terminal, and for each phasor measurement source, as shown in Fig. 4. Due to space limitations, details on the applied PHFL methods are not presented, but their description can be found in [1], [2].

B. Analyzed Power Systems and Fault Scenarios

Fig. 5 shows the analyzed power systems, whose substation are represented by fictitious names (A, B, C, D and E). Fig. 5 also describes the evaluated cases, including information on the real fault distance d, fault type and length L of each analyzed line. These cases consist in real fault scenarios on 500 kV/60 Hz transmission lines, which will be called hereafter TL1, TL2 and TL3. Zero and positive sequence line series impedance settings used in the analyzed PHFL algorithms are shown in Table I, but other details on the evaluated systems are omitted due to confidentiality reasons.

In the next subsections, the above-mentioned fault cases are detailed, presenting also comparative graphics of the FL estimation samples calculated during the fault period when relay and M-class PMU phasor estimations are taken into account. In these graphics, balloons are used to point out the most stable FL estimation sample or those closer to the end of the fault period, which are chosen depending on the presence of oscillations, such as in practical FL procedures.

1) Case 1: BG fault on TL1, d = 37.9 km, L = 343 km: In this case, the fault is at a distance d = 37.9 km from bus A, and $L - d$ = 305.10 km far from substation B. Figs. 6 and 7 show the analyzed records obtained from substations A and B respectively, whereas Figs. 8 and Figs. 9 illustrate the obtained m and ϵ results at each line terminal. It can be seen that the fault duration is of about three power cycles, and that all evaluated PMU-based and relay PHFL results present very similar performances at substation A. On the other hand, at substation B, m_{REL} estimations present relevant oscillations, which in turn are not verified in m_{PMU}. Analyzing these oscillations, it is concluded that they are induced by frequency components present in the evaluated signals, which are not completely eliminated by the relay phasor estimation algorithm. Indeed, besides charging currents and zero sequence mutual coupling with the parallel line, as one can see in Fig. 5, the TL1 is series compensated. Thus, during the fault period, there are sub-synchronous frequencies which aggravate the distortions in the estimated relay phasors [22], yielding also significant oscillations in m_{REL}.

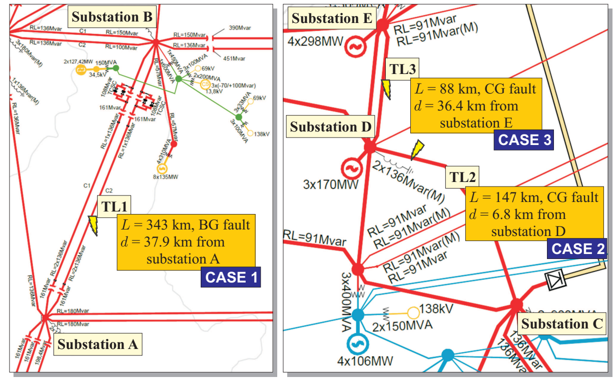

Fig. 5. Tested power systems and case description.

TABLE I
ZERO AND POSITIVE SEQUENCE LINE SERIES IMPEDANCE SETTINGS

Line Code	**Line Series Impedance**	
	Zero Sequence	Positive Sequence
TL1	0.048 + j0.772 Ω/km	0.016 + j0.257 Ω/km
TL2	0.071 + j1.010 Ω/km	0.024 + j0.337 Ω/km
TL3	0.077 + j1.057 Ω/km	0.025 + j0.352 Ω/km

Analyzing substation A data after the stabilization time of FL estimations m, $\epsilon_{REL} < \epsilon_{PMU}$ is verified, being $\epsilon_{REL} \approx 2$ km and $\epsilon_{PMU} \approx 6$ km. On the other hand, at substation B, an average filter had to be applied to m_{REL} samples in order to allow the calculation of a reliable fault distance. Such a procedure is typically used in relay-based PHFL procedures to overcome problems due to oscillations [5]. However, even applying such an additional processing, $\epsilon_{PMU} \approx \epsilon_{REL} \approx 3$ km was obtained, revealing a relatively similar PHFL performance when relay and PMU data were considered, i.e., M-class PMU-based PHFL was feasible.

Still regarding this case, it is noticed that substations A and B presented different ϵ levels. To investigate this fact, the fault resistance was estimated through the method ERI, following guidelines reported in [20]. A fault resistance of about 3 Ω was calculated, in such a way that a slight infeed effect would be expected to occur [1]. Nevertheless, the analyzed PHFL methods apply solutions to reduce the infeed influence [2], bringing the attention to other sources of errors. In this sense, it should be noticed that the TL1 is long (L = 343 km), which results in relevant charging currents that are not compensated by the evaluated PHFL methods [1]. Besides, the system loading and mutual coupling with the parallel circuit are also sources of errors, which can result in different ϵ levels at the monitored line ends, such as verified in this case.

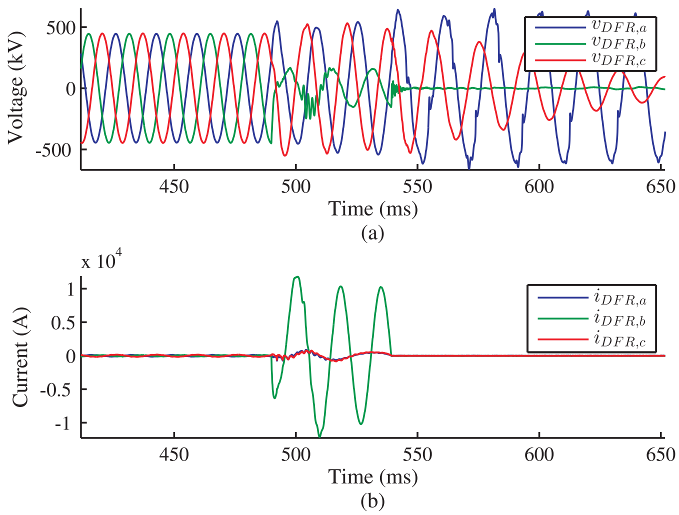

Fig. 6. Case 1 - substation A records: (a) Voltages; (b) Currents.

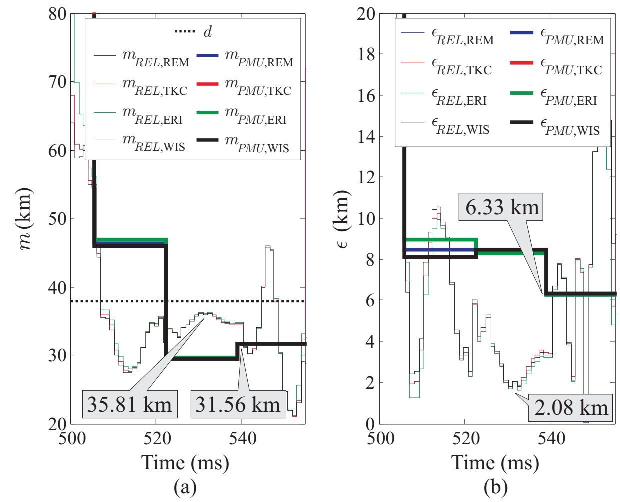

Fig. 8. Case 1 - substation A data analysis: (a) m estimations; (b) ϵ errors.

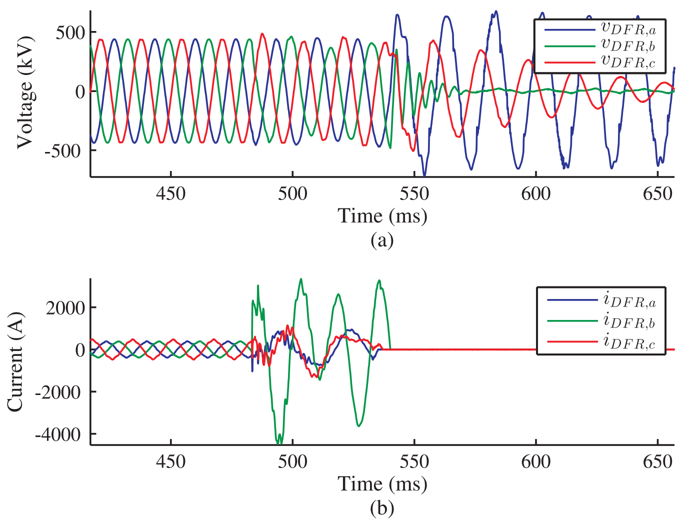

Fig. 7. Case 1 - substation B records: (a) Voltages; (b) Currents.

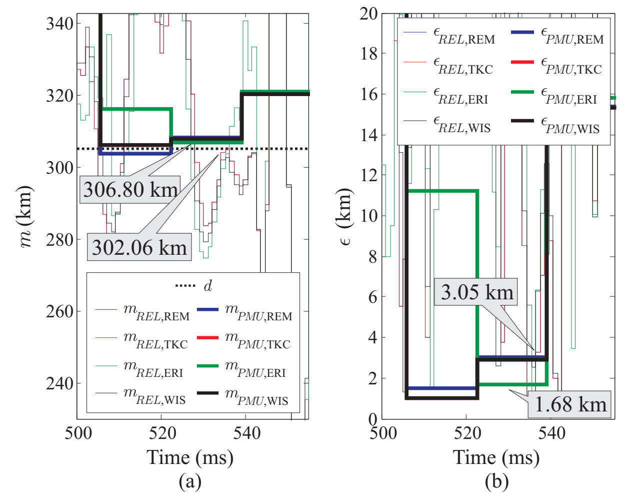

Fig. 9. Case 1 - substation B data analysis: (a) m estimations; (b) ϵ errors.

2) Case 2: CG fault on TL2, $d = 6.8$ km, $L = 147$ km: In this scenario, the fault is at $d = 6.8$ km from substation D, and $L - d = 140.20$ km far away from substation C. Since the transmission line TL2 is not series compensated, the current waveforms behavior is more stable than those observed in Case 1, except by the presence of a relevant decaying DC component. Moreover, similarly to Case 1, the fault duration is of about three power cycles, leading such a scenario to be interesting to evaluate the M-class PMU-based PHFL feasibility. Indeed, in this case, since series compensation is not used, sub-synchronous frequency components are not present in the evaluated waveforms, so that the effects of PMU phasor measurement response times can be evaluated under a less critical scenario regarding the influence of phasor estimation filter frequency response.

The DFR records are presented in Figs. 10 and 11, and the obtained PHFL results are shown in Figs. 12 and 13. Again, m_{REL} and m_{PMU} present quite similar accuracy at both transmission line terminals. Also, m_{PMU} is more stable than m_{REL} at the line terminal farthest from the fault point, i.e., substation C, which is a behavior similar to the one verified in Case 1, but with reduced impact on the FL accuracy. Hence, by applying an average filter to m_{REL} values at bus C, ϵ_{REL} and ϵ_{PMU} did not exceed the order of 2 km at both line terminals, attesting again that the M-class PMU-based PHFL was feasible.

3) Case 3: CG fault on TL3, $d = 36.4$ km, $L = 88$ km: In case 3, the fault is at $d = 36.4$ km from substation E, from where the analyzed records are taken. Figs. 14 and 15 present the analyzed DFR signals and the PHFL obtained results, respectively. Unlike the previous scenarios, it is noticed that currents gradually increase over about six power cycles, from the fault inception until the CBs opening instant. It characterizes a case of varying fault resistance due to burning vegetation, which was confirmed by the line inspection crews and by using the method ERI [20], through which the fault resistance was estimated. As shown in Fig. 16, considering either relay phasors or PMU data, it is concluded that a fault resistance of about 80 Ω is verified at the event beginning,

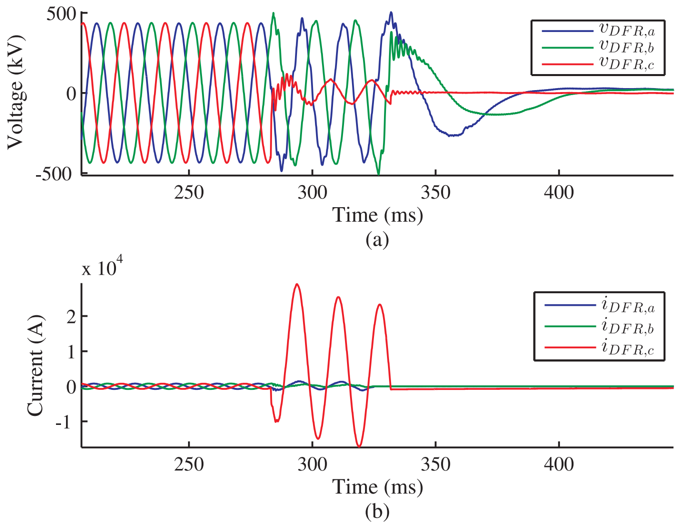

Fig. 10. Case 2 - substation D records: (a) Voltages; (b) Currents.

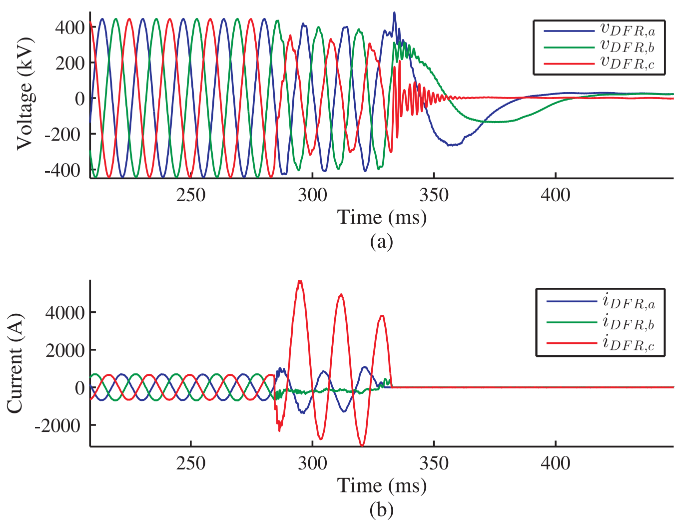

Fig. 11. Case 2 - substation C records: (a) Voltages; (b) Currents.

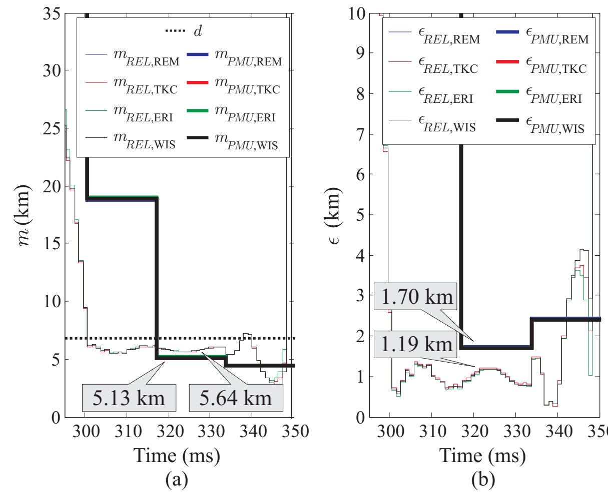

Fig. 12. Case 2 - substation D data analysis: (a) m estimations; (b) ϵ errors.

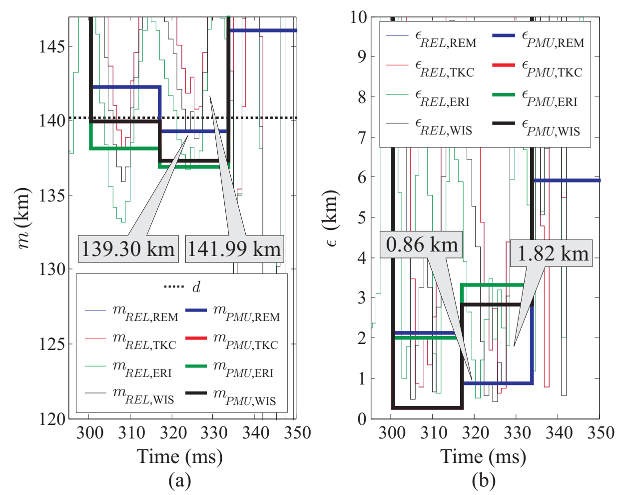

Fig. 13. Case 2 - substation C data analysis: (a) m estimations; (b) ϵ errors.

which reduces to approximately 20 Ω after about six power cycles. Hence, although an infeed effect would be expected, it is compensated by the evaluated PHFL solutions, so that reliable relay and M-class FL estimations could be obtained.

Even with the high fault resistance, ϵ values did not exceed the order of 3.80 km by using the REM method and 1.10 km by using the remaining methods. These performances were verified either using M-class PMU data or relay phasor estimations. Although ϵ_{REL} and ϵ_{PMU} are of the same order, additional oscillations show up in m_{REL}, as in the previous cases, whereas m_{PMU} samples were more stable, despite their delayed response. Even so, m_{REL} oscillations were not critical, since they yielded small FL errors. Moreover, the varying fault resistance did not consist in an obstacle for the PHFL methods when PMU data was used. Therefore, the results attest that, besides resulting in PHFL errors within an acceptable range, the evaluated M-class PMU-based PHFL estimations were more stable those obtained via relay measurements, facilitating the fault diagnosis.

4) Additional Remarks: The analysis of cases 1, 2 and 3 indicate that M-class PMUs can be used in PHFL applications, contrarily to preliminary expectations arising from the well-known M-class PMU phasor estimation delayed response time. Several countries have huge infrastructure of M-class PMUs, but such a promptly available M-class data is often disregarded in PHFL procedures. Hence, clarifying the feasibility of PHFL by using measurements taken from M-class PMUs is of great interest for utilities, such as demonstrated in this paper.

It was shown that, although classical FL methods (like Takagi method and other ones) are usually applied to traditional relay measurements or P-class PMU data, there are evidences that these methods could be also applied considering M-class PMU data. Fault durations ranging from three to six fundamental cycles were verified in the analyzed scenarios, and even with the expected delayed filter response, m_{PMU} estimations were reliable in all cases. Although m_{REL} results were slightly more accurate for faults closer to the monitored terminal in cases 1 and 2, m_{PMU} were more stable, resulting in errors of the same order of those obtained

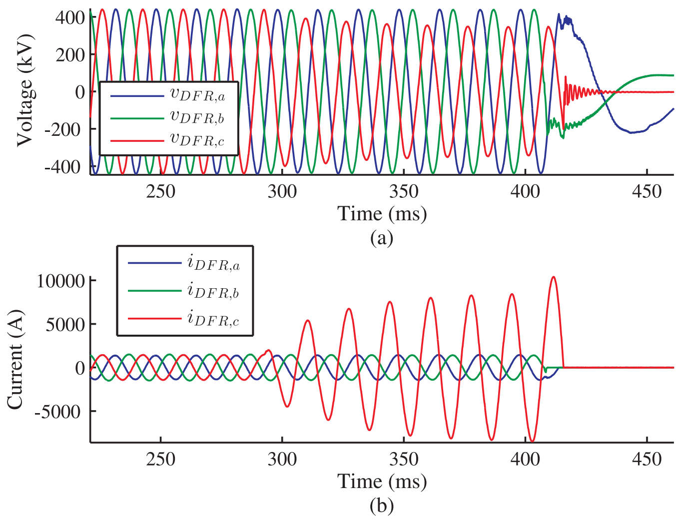

Fig. 14. Case 3 - substation E records: (a) Voltages; (b) Currents.

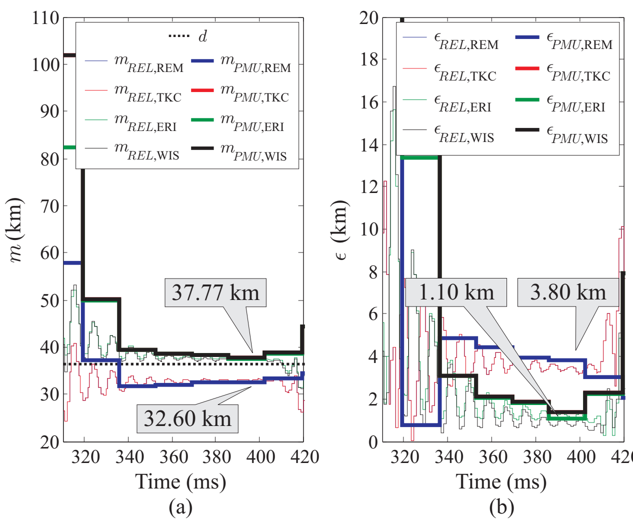

Fig. 15. Case 3 - substation E data analysis: (a) m estimations; (b) ϵ errors.

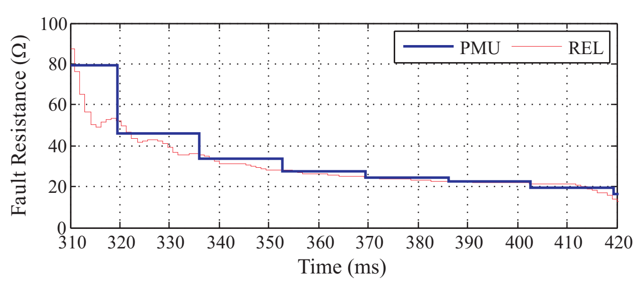

Fig. 16. Case 3 - Estimated fault resistance.

from relay data. Thus, although the authors recognize that further investigation is required, considering other fault types and system operational conditions, the M-class PMU-based PHFL has shown to be feasible in all evaluated events, which opens a promising research topic for future works. Indeed, this conclusion may expand the utilization of M-class PMU networks in several countries, allowing improvements in the currently applied PHFL procedures.

IV. Conclusions

In this work, an innovative study about the feasibility of PHFL methods using phasor data taken from M-class PMUs is presented. Real fault records were analyzed, in such a way that reliable conclusions were drawn overcoming scientific concerns that could arise if simulated records were taken into account. Four different PHFL methods were tested, considering input data taken from PMUs and DFRs installed in the Brazilian power network. In summary, the used phasor inputs were obtained as follows: 1) phasor estimations directly obtained from M-class PMUs; and 2) phasor estimations calculated from a relay algorithm applied to DFR records.

The obtained results show that the evaluated PHFL methods presented very similar performances when M-class PMU and relay phasor estimations were used. It was also observed that the PMU-based fault distance estimations were more stable than those obtained via relay algorithm. It is explained by the improved fundamental component filtering process available in PMUs, despite their larger phasor measurement response times. Thus, unlike the preliminary expectations, it is concluded that there are evidences that some M-class PMUs can be reliably applied in PHFL applications. In Brazil for instance, these results break a paradigm previously established by many professionals, which have considered that the already installed M-class devices could not be used in fault location applications. Hence, although further investigations are required to assess other PMU brands and fault scenarios, a door is now open towards the leverage of the widely available M-class PMU data in fault location schemes, which can be beneficial for several power systems worldwide.

References

[1] M. M. Saha, J. Izykowski, and E. Rosolowski, *Fault Location on Power Networks*, ser. Power Systems. London: Ed. Springer, 2010.

[2] S. Das, S. Santoso, A. Gaikwad, and M. Patel, "Impedance-based fault location in transmission networks: theory and application," *IEEE Access*, vol. 2, pp. 537–557, 2014.

[3] A. G. Phadke and J. S. Thorp, *Computer Relaying for Power Systems*, 2nd ed. New York, USA: John Wiley & Sons Inc, 2009.

[4] K. M. Silva and F. A. O. Nascimento, "Modified dft-based phasor estimation algorithms for numerical relaying applications," *IEEE Transactions on Power Delivery*, vol. 33, no. 3, pp. 1165–1173, 2018.

[5] F. V. Lopes, E. J. S. Leite, J. P. G. Ribeiro, A. B. Piardi, R. G. Fabián Espinoza, A. V. Scheid, G. Zat, and R. B. Otto, "Phasor-based fault location challenges and solutions for transmission lines equipped with high-speed time-domain protective relays," *Electric Power Systems Research*, vol. 189, p. 106617, 2020.

[6] "IEEE standard for synchrophasor measurements for power systems – amendment 1: Modification of selected performance requirements," *IEEE Std C37.118.1a-2014*, pp. 1–25, 2014.

[7] A. Phadke and J. Thorp, *Synchronized Phasor Measurements and Their Applications*. New York: Springer Science & Business Media, 2008.

[8] S. D. Picard, M. G. Adamiak, and V. Madani, "Fault location using pmu measurements and wide-area infrastructure," in *2015 68th Annual Conference for Protective Relay Engineers*, 2015, pp. 272–277.

[9] O. Naidu, P. Yalla, A. Sai, and S. Sawai, "Model-free fault location for transmission lines using phasor measurement unit data," in *Study Committee B5 Colloquium Tromsø, Norway*, 06 2019.

[10] V. Terzija, Z. M. Radojevi?, and G. Preston, "Flexible synchronized measurement technology-based fault locator," *IEEE Transactions on Smart Grid*, vol. 6, no. 2, pp. 866–873, 2015.

[11] T. Becejac, P. Dehghanian, and M. Kezunovic, "Impact of the errors in the pmu response on synchrophasor-based fault location algorithms," in *2016 North American Power Symposium (NAPS)*, 2016, pp. 1–6.

[12] R. A. Guardado and J. L. Guardado, “A pmu model for wide-area protection in atp/emtp,” *IEEE Transactions on Power Delivery*, vol. 31, no. 4, pp. 1953–1960, 2016.

[13] M. Adamiak and B. Kasztenny, “Implementation and performance of synchrophasor function within microprocessor based relays,” *Protection and Control Journal*, p. 35, 2007.

[14] J. R. Razo-Hernandez, A. Mejia-Barron, D. Granados-Lieberman, M. Valtierra-Rodriguez, and J. F. Gomez-Aguilar, “A new phasor estimator for pmu applications: P class and m class,” *Journal of Modern Power Systems and Clean Energy*, vol. 8, no. 1, pp. 55–66, 2020.

[15] W. Meng, X. Wang, Z. Wang, and I. Kamwa, “Impact of causality on performance of phasor measurement unit algorithms,” *IEEE Transactions on Power Systems*, vol. 33, no. 2, pp. 1555–1565, 2018.

[16] “Ieee/iec international standard - measuring relays and protection equipment - part 118-1: Synchrophasor for power systems - measurements,” *IEC/IEEE 60255-118-1:2018*, pp. 1–78, 2018.

[17] D. G. Hart, D. Novosel, and R. A. Smith, *Modified Cosine Filters*, U. S. Patent 6154687 ed., November, 2000.

[18] F. V. Lopes, D. Fernandes, and W. Neves, “A traveling-wave detection method based on Park’s transformation for fault locators,” *IEEE Transactions on Power Delivery*, vol. 28, no. 3, pp. 1626–1634, 2013.

[19] T. Takagi, Y. Yamakoshi, M. Yamaura, R. Kondow, and T. Matsushima, “Development of a new type fault locator using the one-terminal voltage and current data,” *Power Apparatus and Systems, IEEE Transactions on*, vol. PAS-101, no. 8, pp. 2892 –2898, aug. 1982.

[20] L. Eriksson, M. M. Saha, and G. D. Rockefeller, “An accurate fault locator with compensation for apparent reactance in the fault resistance resulting from remote-end infeed,” *IEEE Power Engineering Review*, vol. PER-5, no. 2, pp. 44–44, 1985.

[21] A. Wiszniewski, “Accurate fault impedance locating algorithm,” *Generation, Transmission and Distribution, IEE Proceedings C*, vol. 130, no. 6, pp. 311 –314, november 1983.

[22] D. Moura, F. Moreira, and K. Silva, “Effects of subharmonic frequencies in phasor estimation algorithms for distance protection of series compensated transmission lines,” in *10th International Conference in Power Systems Transients, Vancouver, Canada*, 2013.